



Anomalous coherence length of Majorana zero modes at vortices in superconducting topological insulators

Bo Fu  and Shun-Qing Shen *Department of Physics, The University of Hong Kong, Pokfulam Road, Hong Kong, China* (Received 14 December 2022; revised 16 May 2023; accepted 17 May 2023; published 30 May 2023)

The coherence length of two Majorana zero-energy modes in a p -wave topological superconductor is inversely proportional to the superconducting order parameter. We studied the finite size effect of the Majorana zero modes at vortices in a topological insulator/superconductor heterostructure in the presence of a vortex and found that the coherence length of the two zero-energy modes at the terminals of a vortex line is independent of the superconducting order parameter and determined by the intrinsic properties of the topological insulator. This anomalous property illustrates that the superconducting topological insulator is topologically distinct, contrary to a p -wave topological superconductor.

DOI: [10.1103/PhysRevB.107.184517](https://doi.org/10.1103/PhysRevB.107.184517)

I. INTRODUCTION

The search for Majorana zero modes in topological phases has generated extensive interest in condensed matter physics and material science [1–8]. The Majorana zero modes in a topological superconductor carry zero energy and obey non-Abelian statistics. Their occupancy can form the topological degeneracy of the ground states of the system, which are expected to have potential application for fault tolerant topological quantum computation [9–11]. In their pioneering work, Fu and Kane [12] proposed that the proximity effect between an s -wave superconductor and the surface electrons of a strong topological insulator leads to a time-invariant superconducting state resembling a spinless $p_x \pm ip_y$ superconductor. They proposed that this interface supports Majorana bound modes at vortices. Over the past decade, this proposal has attracted significant attention and become one of the main prototypes to construct and to engineer a physical system to host the topological excitations [13–22] and to understand the zero-energy modes observed in iron-based superconductors [23–35]. However, the search for Majorana zero modes is meeting great difficulty and challenge especially in experiments.

The time-reversal-invariant superconductor with spin-orbit coupling belongs to symmetry class DIII and in two dimensions is characterized by a \mathbb{Z}_2 topological invariant [36–38]. The topologically nontrivial phase hosts a pair of helical Majorana modes on its edge [39–42]. Theoretically, it can be realized by considering the spin-triplet superconducting pairing with odd-parity or extended- s -wave pairing which flips its sign when it evolves across the Brillouin zone. Based on the odd-parity superconductivity criterion [40,43], the strong topological insulator in contact with an s -wave superconductor is topologically trivial without edge modes, which is distinctly different from the chiral p -wave topological superconductor [44,45]. The existence of the zero-energy vortex mode in this system is associated with the Atiyah-Singer index theorem which clarifies the correspondence between the vorticity of the vortex and the number of the localized

zero-energy modes for the surface states [46–48]. It heavily relies on the validity of the topological insulator's surface states and the presence of the chiral symmetry. Furthermore, the chemical potential enters into the Bogoliubov–de Gennes (BdG) equation in a nontrivial way and breaks the chiral symmetry explicitly that the index theorem does not apply here. There arises the question of how the tunneling between two surfaces lifts the degeneracy of the Majorana modes in a thin film for a finite chemical potential.

In the present work, we investigate the finite size effect of the Majorana zero-energy modes in vortices in the topological insulator/superconductor (TI/SC) heterostructure depicted as Fig. 1(a). In the presence of the superconducting vortex the two Majorana modes are present and connected through the bulk topological insulator along the vortex when the chemical potential μ is lower than a critical value $\mu < \mu_c$. The energy splitting of the two modes decays exponentially with the thickness and the coherence length only depends on the intrinsic properties of the topological insulator and is independent of the superconducting order parameter. As a comparison, we also present the results for the semi-magnetic topological insulator/superconductor (SMTI/SC) heterostructure depicted as Fig. 2(a), which is equivalent to a p -wave topological superconductor when the chemical potential locates within the magnetic gap of the top surface states. The two Majorana modes reside at the vortex core and at the boundary separately and their coherence length is equal to the superconducting coherence length, which is a typical signature of a p -wave topological superconductor. Thus the anomalous coherence length in the TI/SC heterostructure indicates that the pair of the zero-energy modes at the vortex core is attributed to the winding number of the superconducting order parameter, not to the p -wave topological superconductivity.

II. TI/SC HETEROSTRUCTURE

We start with a minimal bulk model for a three dimensional topological insulator $H_{\mathbf{k}}$ which supports gapless surface

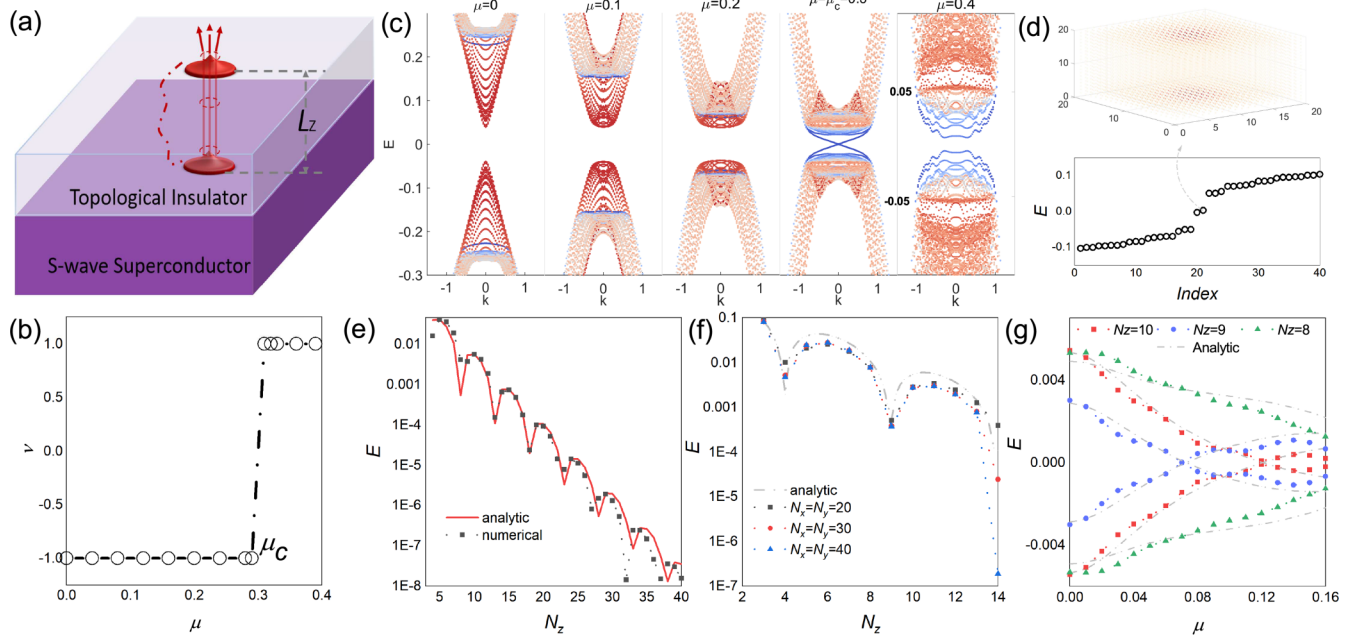


FIG. 1. TI/SC heterostructure in the presence of a superconducting vortex. (a) Schematic with two zero-energy modes bound to a vortex line. L_z denotes the thickness of the sample. (b) \mathbb{Z}_2 topological invariant as a function of μ . (c) The dispersions of a quasi-1D system at different values of μ . The blue-to-red color gradient indicates the radial probability distribution for each band with the vortex line at the origin. The blue colored bands correspond to the dispersions for the vortex bound states. (d) Energy spectrum and the wave function for the zero-energy modes for open boundary conditions. (e) Plot of the finite size induced gap between the surface states at $k_x = k_y = 0$ as a function of the thickness $L_z = N_z a$ with a as the lattice constant. (f) For $\mu = 0$, the evolution of the energy of the vortex bound states with respect to the thickness N_z . (g) The energies of the vortex states as a function of μ . For $N_z = 8$, $N_x = N_y = 50$ and for $N_z = 9, 10$, $N_x = N_y = 40$. Parameters are $\Delta = 0.05$, $\hbar v = 0.4$, $B = 0.5$, and $m = 0.28$.

states [3]. The numerical calculation is based on a tight-binding model on a cubic lattice and the analytical study is based on the continuum model in the long wavelength approximation that the lattice Hamiltonian is expanded in terms of the wave vector \mathbf{k} to the second order around Γ point, $H_{\mathbf{k}} = v\rho_x \mathbf{k} \cdot \boldsymbol{\sigma} + M(\mathbf{k})\rho_z - \mu$, where $M(\mathbf{k}) = m - B\mathbf{k}^2$, the Pauli matrices σ and ρ are acting on spin and orbit space, respectively [3,5,49], v , m , B are the material parameters, and μ is the chemical potential. In proximity to an s -wave superconductor, a finite superconducting pairing Δ is induced in the three-dimensional topological insulator, which leads to the BdG Hamiltonian $H_{\mathbf{k}}^{\text{BdG}}$. Based on the odd-parity superconductivity criterion, $H_{\mathbf{k}}^{\text{BdG}}$ is topologically trivial without gapless edge modes around the system [40]. In the presence of a vortex in z direction, $\Delta \rightarrow \Delta(r)e^{i\theta}$, with (r, θ) as the in-plane polar coordinates with respect to the vortex core, the translational invariance along z direction persists, and k_z is still a good quantum number. The problem becomes classifying the gapped phases in quasi-1D whose unit cell consists of all the sites in xy plane. Due to the lack of time reversal symmetry, it belongs to symmetry class D and is characterized by a \mathbb{Z}_2 invariant ν , which is defined as the product of signs of Pfaffians of the antisymmetric and real BdG Hamiltonians in the Majorana representation at two time reversal invariant momenta $k_z = 0, \pi$ [37,50]. With increasing μ , the quasi-1D system transitions into the trivial phase via a quantum critical point $\mu = \mu_c \simeq v\sqrt{\frac{m}{B}}$ at which ν changes from -1 to $+1$ as shown in Fig. 1(b). In Fig. 1(c), we also present the numerical results of the evolution of the dispersion under the variation of

μ . The results reveal that the vortex line is fully gapped except at $\mu = \mu_c$, where a vortex phase transition takes place [51]. For $\nu = -1$ ($\mu < \mu_c$), the quasi-1D system is topological nontrivial and there exists a single 0D zero mode at each end of the termination along z direction [51,52] as shown in Fig. 1(d). In order to estimate the energy splitting of two vortex line end states for finite thickness L_z , we derive the effective Hamiltonian for the vortex line. By projecting onto the two states centered at the vortex line which is denoted by the darkest of blue color in Fig. 1(c), we obtain the effective dispersions (see Appendix B)

$$H_{\text{eff}} = -\mathcal{F}(k_F^2 \xi^2) [(\tilde{m} - Bk_z^2)v_z + vk_z v_y], \quad (1)$$

where $\tilde{m} = m - Bk_F^2 - \frac{B}{\xi^2}$ is the renormalized mass with $k_F = \mu/v$ and $\xi = v/\Delta$, v_i are Pauli matrices acting on the projected two bands, and $\mathcal{F}(x) = [-\frac{E(-x)}{x+1} + K(-x)]/[E(-x) - K(-x)]$ is a monotonically decreasing function, where K and E are the complete elliptic integral of the first and second kind, respectively. The superconducting pairing only enters into an overall energy renormalization function \mathcal{F} , which can be factored out without changing any of the topological properties. Then, the effective Hamiltonian (1) resembles the 1D Su-Schrieffer-Heeger model [53] instead of the 1D topological Kitaev chain in which the p -wave pairing is linear in momentum [54]. Consequently, when $\tilde{m}B > 0$, the vortex line Hamiltonian is topologically nontrivial. At $\tilde{m} = 0$, which corresponds to a critical chemical $\mu = \mu_c$, the gap vanishes, signaling a topological phase transition which is consistent

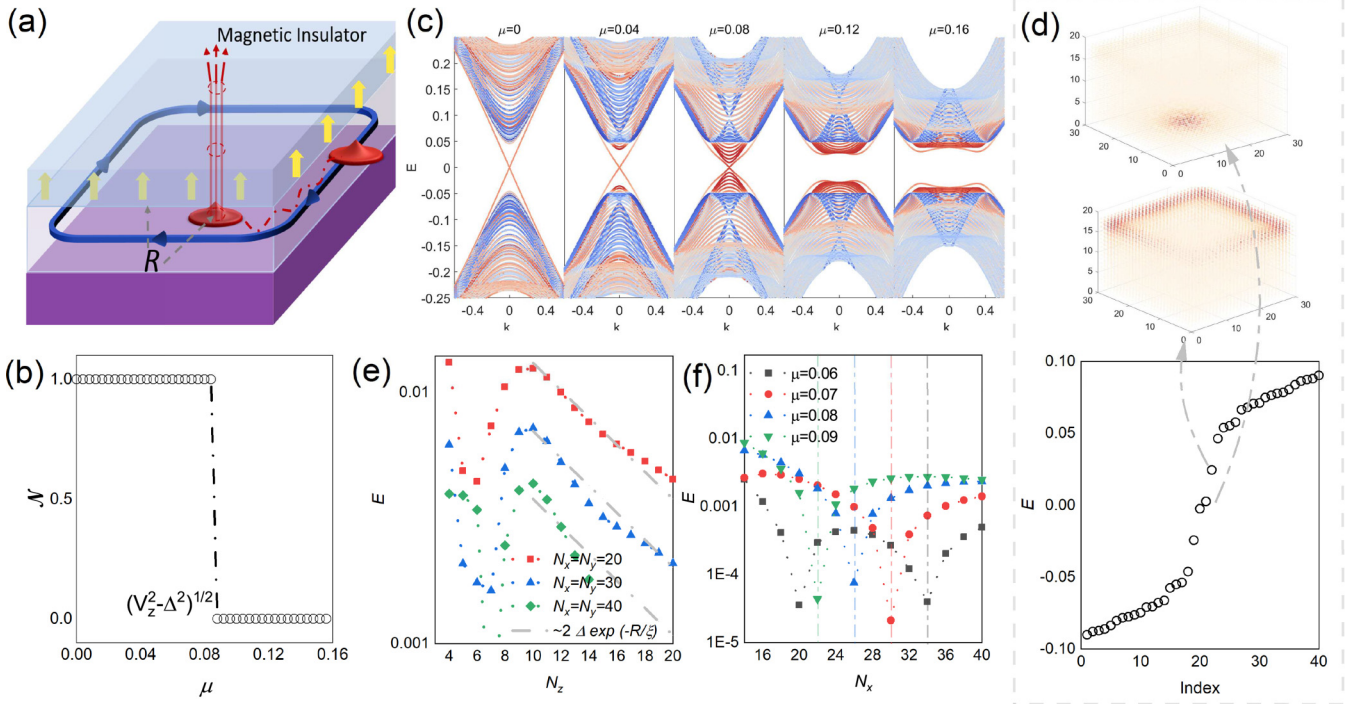


FIG. 2. SMTI/SC heterostructure. (a) Schematic of the zero-energy modes residing in the vortex core and the boundary. (b) In the absence of vortex, the Chern number \mathcal{N} of the quasi-2D system as a function of μ . (c) The quasi-one-dimensional band structure for μ for $N_z = 10$ and $N_y = 100$. The distribution of the wave function along the z direction indicated by the scale from blue to yellow color. (d) The energy spectra for the open boundary condition and the illustration of the spatial probability distribution $|\Psi(x, y, z)|^2$ of zero-energy state and the chiral state for a $30 \times 30 \times 18$ lattice. (e) At $\mu = 0$, the energy for the lowest energy mode as a function of N_z for different N_x and N_y . (f) For finite μ , the energy for the lowest energy mode as a function of N_x and N_y for $N_z = 10$. The singularity points in the logarithmic plot due to the oscillation are indicated by the vertical dashed lines. Parameters are $\Delta = 0.05$, $\hbar v = 0.4$, $b = 0.5$, and $m = 0.28$. The exchange field $V_z = 0.1$ is added to top three layers.

with the \mathbb{Z}_2 topological invariant. From Eq. (1), we can obtain the energy splitting for the zero-energy modes

$$\delta E = \frac{4\tilde{m}v\mathcal{F}(k_F^2\xi^2)}{\sqrt{4B\tilde{m}-v^2}} \left| \sin\left(\frac{\sqrt{4\tilde{m}B-v^2}}{2B}L_z\right) \right| \exp\left(-\frac{vL_z}{2B}\right). \quad (2)$$

For the chemical potential $\mu \sim 0$ or in the strong pairing limit $k_F\xi \ll 1$, we have $\mathcal{F}(k_F^2\xi^2) \simeq 1$ and $\tilde{m} \simeq m$; the energy splitting is independent on the superconducting pairing and recovers the finite size effect for the surface state of topological insulator [55,56]. As shown in Fig. 1(f), the energy splitting of the zero-energy states based on tight-binding numerical calculations quickly saturates when the size of the slab is much larger than the superconducting coherence length $L_x, L_y \gg \xi$ and features an oscillating exponential decay with increasing the thickness of the sample, which agrees well with the analytic expression. For $\mu \neq 0$, since the chemical potential enters into the oscillating function $\sin\left(\frac{\sqrt{4\tilde{m}B-v^2}}{2B}L_z\right)$ through the renormalized mass \tilde{m} , the energy splitting is also sensitive to μ besides the thickness of the sample as shown in Fig. 1(g). For large μ or the weak pairing limit $k_F\xi \gg 1$, $\mathcal{F}(k_F^2\xi^2) \simeq \frac{\ln(4k_F\xi)-1}{k_F^2\xi^2}$ shows a power-law decrease of $k_F\xi$. Due to the presence of this prefactor, the finite size effect is strongly suppressed.

This energy splitting can be understood from aspects of top and bottom surface states with superconducting pairing by means of the index theorem [57–59]. The Dirac surface states of strong topological insulator thin films can be described by $h_{\mathbf{k}_i}^{\text{surf}} = vQ_z(\mathbf{k}_i \times \boldsymbol{\sigma})_z + tQ_x - \mu$, where $\mathbf{k}_i = (k_x, k_y, 0)$ denotes the in-plane wave vector, t is the intersurface tunneling, and the Pauli matrices Q and σ denote surface and spin degrees of freedom, respectively. In combination with the superconducting pairing, the BdG Hamiltonian is $H_{\text{BdG}}^{\text{surf}}(\mathbf{k}_i) = \tau_z h_{\mathbf{k}_i}^{\text{surf}} + \Delta\tau_x$, which belongs to the Altland-Zirnbauer symmetry class DIII and is classified by a \mathbb{Z}_2 topological invariant. This system has the mirror symmetry $M_z = iQ_x\sigma_z$ with $M_z^2 = -1$, which reflects the top surface to the bottom surface. After a uniform $\pi/2$ rotation around $Q_y\sigma_z$, the full BdG Hamiltonian can be decoupled into the direct sum of two mirror sectors $H_{\mathbf{k}_i}^X$ with mirror eigenvalue as $i\chi$. The two subblocks are particle-hole partners of each other: $\tau_y\sigma_x H_{\mathbf{k}_i}^{X*}\sigma_x\tau_y = -H_{-\mathbf{k}_i}^{-X}$. Each subblock breaks particle-hole symmetry explicitly and possesses the chiral symmetry $\{\mathcal{C}, H_{\mathbf{k}_i}^X\} = 0$ with $\mathcal{C} = \tau_y$ and thus belongs to the class AIII. In two spatial dimensions, the topological classification for class AIII is trivial [36]. In the presence of a vortex, the pertinent Hamiltonian for $\mu = 0$ becomes

$$H^X = \chi\tau_z[-iv(\sigma_y\partial_x - \sigma_x\partial_y) + t\sigma_z] + \Delta(\cos\theta\tau_x + \sin\theta\tau_y), \quad (3)$$

where \mathbf{k}_\parallel is replaced by $-i(\partial_x, \partial_y)$. Note that the five four-dimensional Hermitian matrices anticommute with each other and the interface tunneling term enters into the Hamiltonian as the fifth anticommuting matrix. For $t = 0$, there is additional chiral symmetry $\tau_z \sigma_z$ in H^χ , which can be expressed as $\{\tau_z \sigma_z, H^\chi\} = 0$ and ensures the spectral symmetry. As a consequence, the zero-energy states $|\Psi_0^\chi\rangle$ of H^χ becomes eigenstates of $\tau_z \sigma_z$ with eigenvalue as ± 1 . The analytic index of the chiral symmetric model is defined by $\text{ind} H^\chi = n_+ - n_-$, where n_\pm are the number of zero-energy states with chirality ± 1 . The index theorem states that the analytic index is identical to the winding number of the order parameter in the two-dimensional space and there are exactly n number of zero modes for the vorticity n [57–59]. Also, as pointed in Ref. [60], the zero modes are associated with hedgehogs in the complex vector fields of the superconducting order parameter $\mathbf{n}(\mathbf{r}) = (\Delta \cos \theta, -\Delta \sin \theta)$. In particular, when the vorticity is one there exists a single state at zero energy for H^χ . After including the chirality symmetry breaking term $\chi t \tau_z \sigma_z$, we have $(H^\chi + \chi t \tau_z \sigma_z)|\Psi_0^\chi\rangle = \chi t \tau_z \sigma_z |\Psi_0^\chi\rangle = \chi t |\Psi_0^\chi\rangle$ that the energy will be shifted from zero to χt . The existence of the zero-energy solution heavily relies on the assumption that the intersurface tunneling is negligible. When the tunneling effects are taken into account, the zero-energy bound states are actually shifted away from zero.

III. SMTI/SC HETEROSTRUCTURE

For comparison, we now turn to the SMTI/SC heterostructure. The exchange interaction between the magnetic ion and the surface electrons leads to nonzero magnetization and makes the top surface electrons open an energy gap $2|V_z|$. When the Fermi level intersects gapless bottom surface states and locates within the magnetic gap of the top surface states, i.e., $|\mu| < \sqrt{V_z^2 - \Delta^2}$, the quasi-2D system is topologically equivalent to a chiral topological superconductor with nonzero Chern number supporting chiral Majorana modes on its boundary [12,61–69]. A topological phase transition occurs at $|\mu| = \sqrt{V_z^2 - \Delta^2}$ in Fig. 2(b). It is verified by numerical calculations for different μ as shown in Fig. 2(c). The presence of edge states is consistent with the bulk band topology. After introducing a vortex, the existence of the Majorana zero-energy state is governed by the BdG Hamiltonian for the surface states. We then map the surface states onto a 2D plane with the intersection point of the vortex line with the bottom surface mapped to the center of the plane. In this situation, the exchange field only exists outside a disk radius R , i.e., $M(r) = V_z \Theta(r - R)$. For $\sqrt{V_z^2 - \Delta^2} > \mu > 0$, we find a zero-energy solution $|\psi_{\text{core}}\rangle$ localized at the vortex core and a bound state $|\psi_{\text{inter}}\rangle$ localized at the interface between the magnetic and nonmagnetic regions [44,45,70]. We can construct the approximate eigenstate wave function as $|\Psi_\pm\rangle = \frac{1}{\sqrt{2}}(|\psi_{\text{core}}\rangle \pm |\psi_{\text{inter}}\rangle)$ with the energies $E_+ = -E_- = \delta E$ [71,72]. These two wave functions satisfy the particle-hole symmetry of the BdG equations, $\Xi|\Psi_+\rangle = |\Psi_-\rangle$. As shown in Fig. 2(d), based on the tight binding calculations, we present the energy spectra and the wave functions for the lowest two energy states. The zero-energy state is constituted by two parts of contributions: one part is exponentially localized at the vortex core, while the other part is localized at the interface.

In addition to the zero modes, there are chiral modes peaked only at the interface within the superconducting gap. By considering the overlapping of two zero-energy modes, the energy splitting can be obtained as (Appendix C)

$$\delta E \approx 2\Delta e^{-R/\xi} |\sin(k_F R - \delta)|, \quad (4)$$

where $\delta = \arctan \sqrt{\frac{V_z + \mu}{V_z - \mu}} + \frac{\pi}{4}$. The energy splitting decays exponentially as a function of R . The coherence length is simply the superconducting coherence length $\xi = v/\Delta$, which is proportional inversely to the superconducting order parameter Δ . The analytic result (4) is in qualitative agreement with the numerical results as shown in Figs. 2(e) and 2(f).

In order to gain better insight into the difference between the two present cases, we derive an effective model to capture the main physics in the SMTI/SC heterostructure. We start from the effective Hamiltonian for the strong topological insulator thin films in contact with the magnetic insulator on its top, $h_{\mathbf{k}_\parallel}^{\text{mag}} = -v(\mathbf{k}_\parallel \times \boldsymbol{\sigma})_z + M(\mathbf{k}_\parallel)\sigma_z$ [73,74]. At low energy ($k_\parallel < k_c$ with $k_c \simeq \sqrt{\frac{m}{B}}$), $M(\mathbf{k}_\parallel) = 0$, $h_{\mathbf{k}_\parallel}^{\text{mag}}$ turns out to be the massless Dirac Hamiltonian which describes the bottom surface states. At high energy regime ($k_\parallel > k_c$), $M(\mathbf{k}_\parallel) \neq 0$ originates from the surface states that evolve into the bulk in the high energy regime and break time reversal symmetry explicitly. Thus $M(\mathbf{k}_\parallel)$ behaves as a regularization term and changes the band topology. The wave function with the positive eigenvalue can be solved as $|\psi_c\rangle = (i \cos \frac{\varphi_{\mathbf{k}_\parallel}}{2}, e^{i\theta_{\mathbf{k}_\parallel}} \sin \frac{\varphi_{\mathbf{k}_\parallel}}{2})$ for $M(\infty) > 0$ and $|\psi_c\rangle = (i e^{-i\theta_{\mathbf{k}_\parallel}} \cos \frac{\varphi_{\mathbf{k}_\parallel}}{2}, \sin \frac{\varphi_{\mathbf{k}_\parallel}}{2})$ for $M(\infty) < 0$, where $\cos \varphi_{\mathbf{k}_\parallel} = M(\mathbf{k}_\parallel)/\epsilon(\mathbf{k}_\parallel)$ with $\epsilon(\mathbf{k}_\parallel) = \sqrt{v^2 k_\parallel^2 + M^2(\mathbf{k}_\parallel)}$. Note that the angular factor $e^{\pm i\theta}$ must accompany the component vanishing at $k_\parallel \rightarrow \infty$ to ensure the single valuedness of the wave function. After the inclusion of the superconducting pairing, the BdG Hamiltonian can be projected onto the two bands which are intersected with the Fermi energy,

$$H_{\text{BdG}}^{\text{mag}} = \begin{pmatrix} \epsilon(\mathbf{k}_\parallel) - \mu & \frac{v k_\parallel}{\epsilon(\mathbf{k}_\parallel)} \Delta e^{-\text{sgn}[M(\infty)]i\theta_{\mathbf{k}_\parallel}} \\ \frac{v k_\parallel}{\epsilon(\mathbf{k}_\parallel)} \Delta e^{\text{sgn}[M(\infty)]i\theta_{\mathbf{k}_\parallel}} & -\epsilon(\mathbf{k}_\parallel) + \mu \end{pmatrix}. \quad (5)$$

It is an effective chiral p -wave BdG Hamiltonian and the chirality crucially depends on the sign of the $M(\infty)$. The projected Hamiltonian cannot be determined without ambiguity in the absence of the regulator. The Chern number for the occupied band is $\mathcal{N} = \text{sgn}[M(\infty)]$. The presence of a vortex will lead to the antiperiodical condition for the wave function, $\Psi(r, \theta + 2\pi) = e^{i\pi} \Psi(r, \theta)$ [44,45]. By using the ansatz for the wave function $\Psi_l(\mathbf{r}) = \frac{e^{i\theta}}{\sqrt{2\pi r}} [e^{-i\theta/2} u_l(r), e^{i\theta/2} v_l(r)]$, we can obtain the radial BdG Hamiltonian for $[u_0(r), v_0(r)]$,

$$H_{\text{BdG}}^{\text{radial}} = [\epsilon(-\partial_r^2) - \mu] \tau_z - i \frac{\Delta}{2\mu} v \partial_r \tau_x,$$

which is equivalent to a 1D Kitaev chain. The superconducting pairing only enters into the off-diagonal terms in sharp contrast with Eq. (1).

IV. SUMMARY

The pairing patterns of the Majorana modes in the TI/SC and SMTI/SC heterostructure in the presence of a vortex

have different features. Both numerical simulation and analytical analysis show that the energy splitting of the modes decays exponentially in the thickness L_z of the TI layer in the TI/SC structure and the size R of the SMTI/SC structure. The coherence length in the TI/SC is independent of the superconducting order parameter, which is contrary to that in the SMTI/SC structure or a p -wave topological superconductor. The distinct behaviors of the coherence lengths in two cases reveal that the microscopic origins and the topological nature of the vortex Majorana zero modes are different.

ACKNOWLEDGMENTS

This work was supported by the National Key R&D Program of China under Grant No. 2019YFA0308603 and the Research Grants Council, University Grants Committee, Hong Kong under Grants No. C7012-21GF and No. 17301220.

APPENDIX A: TIGHT-BINDING MODEL FOR NUMERICAL SIMULATIONS

In this section, we give the explicit model for the tight-binding calculations. The microscopic model for the bulk model of the hybrid system with a single vortex is defined by the Hamiltonian,

$$\hat{H}_{\text{tot}} = \hat{H}_{\text{TI}} + \hat{H}_{\text{SC}} + \hat{H}_Z.$$

The \hat{H}_{TI} term describes the topological electronic structure of the bulk system. In the basis of $|P1_z^+, \uparrow\rangle$, $|P1_z^+, \downarrow\rangle$, $|P2_z^-, \uparrow\rangle$, $|P2_z^-, \downarrow\rangle$, it can be written as [3,5,49]

$$\begin{aligned} \hat{H}_{\text{TI}} = & \sum_{\mathbf{r}} \psi_{\mathbf{r}}^\dagger \left[\left(M - \sum_{\delta} B_{\delta} \right) \rho_z \sigma_0 - \mu \rho_0 \sigma_0 \right] \psi_{\mathbf{r}} \\ & + \sum_{\mathbf{r}, \delta} \left[\psi_{\mathbf{r}}^\dagger \frac{1}{2} \left(B_{\delta} \rho_z \sigma_0 - \frac{iv_{\delta}}{a} \rho_x \sigma_{\delta} \right) \psi_{\mathbf{r}+\delta} + \text{H.c.} \right], \end{aligned}$$

where ρ_i and σ_i ($i = 0, x, y, z$) are Pauli matrices acting on the orbit and spin spaces, respectively. $\psi_{\mathbf{r}} = [c_{\mathbf{r}1\uparrow}, c_{\mathbf{r}1\downarrow}, c_{\mathbf{r}2\uparrow}, c_{\mathbf{r}2\downarrow}]^T$ are annihilation operators of the four-component spinor at position \mathbf{r} . $2M$ is the band gap at Γ point. $\frac{\hbar}{a}v_{\delta}$ and B_{δ} describe the spin-dependent and spin-independent hoppings on the cubic lattice along the δ direction with $\delta = x, y, z$. a is the lattice constant. μ is the chemical potential. For simplicity, we take $B_x = B_y = B_z = B$; then the above model describes a strong topological insulator phase with gapless surface states for $2 > M/B > 0$.

The proximity-induced superconductivity \hat{H}_{SC} can be described by

$$\hat{H}_{\text{SC}} = \sum_{\mathbf{r}} [\psi_{\mathbf{r}}^\dagger \Delta(\mathbf{r}) e^{-i\phi(\mathbf{r}_{\parallel})} i\sigma_y \psi_{\mathbf{r}} + \text{H.c.}],$$

where $\phi(\mathbf{r}_{\parallel}) = \arg(\mathbf{r}_{\parallel} - \mathbf{r}_{\parallel}^0)$, with $\mathbf{r}_{\parallel} = (x, y)$ as the planar position vector, \mathbf{r}_{\parallel}^0 as the coordinate for the vortex line, and \arg representing the argument of the vector. The pairing function is written as $\Delta(\mathbf{r}) = \Delta_0 f(z) \tanh(r_{\parallel}/\xi)$, where Δ_0 is the amplitude of the pairing function, $f(z)$ and $\tanh(r_{\parallel}/\xi)$ are the distribution function along z and the planar direction,

respectively, and $\xi = v/\Delta_0$ is the coherent length of the superconductor. Here we think the thickness of the topological insulator film is much less than the coherent length of the superconductor such that $f(z) \simeq 1$.

\hat{H}_Z describes the Zeeman term which is modeled as

$$\hat{H}_Z = \sum_{\mathbf{r}} V_z(z) \psi_{\mathbf{r}}^\dagger \rho_0 \sigma_z \psi_{\mathbf{r}},$$

with V_z as the amplitude of the exchange field. The exchange field is only restricted to several layers near the top surface of the system, $V_z(z) = V_z \Theta(z_m - z)$, where Θ is the Heaviside step function and z_m is the thickness of magnetic layers.

APPENDIX B: DERIVATION OF THE EFFECTIVE VORTEX HAMILTONIAN

The inclusion of the s -wave superconductivity in the three-dimensional topological insulator leads to the Bogoliubov–de Gennes (BdG) Hamiltonian as

$$H_{\mathbf{k}}^{\text{BdG}} = \begin{pmatrix} H_{\mathbf{k}} & \Delta \\ \Delta & -\sigma_y H_{-\mathbf{k}}^* \sigma_y \end{pmatrix},$$

where Δ is the superconducting pairing. In the presence of a vortex in z direction, the superconducting pairing $\Delta \rightarrow \Delta(r)e^{i\theta}$ with respect to the vortex core. We have used cylindrical coordinates $(x, y, z) = (r \cos \theta, r \sin \theta, z)$. In view of the rotational symmetry about the z axis, we can assign the quantum numbers (k_z, l, n) for the bulk of the system, which are the momentum in z direction, the angular momentum in xy plane, and the radial quantum number, respectively. These emergent symmetries of the effective Hamiltonian allow us to obtain the radial BdG equation $H_{k_z, l}^{\text{BdG}} \Psi_{k_z, l, n} = E_{k_z, l, n} \Psi_{k_z, l, n}$ at a given k_z and l with

$$H_{k_z, l}^{\text{BdG}} = \begin{pmatrix} H_{k_z, l} & \Delta(r) \\ \Delta(r) & -\sigma_y H_{-k_z, -l}^* \sigma_y \end{pmatrix},$$

where

$$H_{k_z, l} = \begin{pmatrix} M_{k_z}^{1-l} - \mu & 0 & vk_z & -viD_r^l \\ 0 & M_{k_z}^l - \mu & -viD_r^{1-l} & -vk_z \\ vk_z & -viD_r^l & -M_{k_z}^{1-l} - \mu & 0 \\ -viD_r^{1-l} & -vk_z & 0 & -M_{k_z}^l - \mu \end{pmatrix}.$$

Here we have introduced $D_r^l = \partial_r + l/r$ and $M_{k_z}^l = m - Bk_z^2 + BD_r^{1-l}D_r^l$. To find the effective Hamiltonian for the vortex line, we first rewrite the Hamiltonian as $H(k_z, l) = H_1(\partial_r, l) + H_2(k_z, l)$, then solve solutions for k_z -independent part H_1 , and finally project k_z -dependent part H_2 onto the relevant bands. H_1 can be expressed as a direct sum of $+$ and $-$ sectors $H_1^{\pm}(\partial_r, l) = -iv(\partial_r + \frac{1}{2r})\tau_z v_x - \mu\tau_z + \Delta(r)\tau_x \mp \frac{v}{2r}\tau_0 v_y \pm \frac{vl}{r}\tau_z v_y$. For $l = 0$, there exists a chiral symmetry $\tau_y v_x H_1^{\pm}(\partial_r, l = 0)\tau_y v_x = -H_1^{\pm}(\partial_r, l = 0)$, which plays an essential role in the determination of the zero-energy solutions.

The zero-energy solutions for H_1^\pm can be solved as

$$|\phi_+\rangle = N e^{-\int_0^r dr' \frac{\Delta(r')}{v}} \begin{pmatrix} -J_1(k_F r) \\ 0 \\ 0 \\ iJ_0(k_F r) \\ J_0(k_F r) \\ 0 \\ 0 \\ iJ_1(k_F r) \end{pmatrix},$$

$$|\phi_-\rangle = N e^{-\int_0^r dr' \frac{\Delta(r')}{v}} \begin{pmatrix} 0 \\ J_0(k_F r) \\ iJ_1(k_F r) \\ 0 \\ 0 \\ J_1(k_F r) \\ -iJ_0(k_F r) \\ 0 \end{pmatrix},$$

with the normalization factor defined as

$$4\pi N^2 \int_0^\infty dr r e^{-2\int_0^r dr' \frac{\Delta(r')}{v}} [J_0^2(k_F r) + J_1^2(k_F r)] = 1.$$

The expectation values of the remaining terms in H_2 with respect to the zero-energy solutions for H_1^\pm can be calculated as

$$\langle \phi_s | \mathcal{M}_{k_z}^0 | \phi_{s'} \rangle = s \delta_{ss'} \mathcal{F}(k_z^2 \xi^2) \left[m - B \left(k_z^2 + k_F^2 + \frac{1}{\xi^2} \right) \right],$$

$$\langle \phi_s | v k_z \tau_z \rho_x \sigma_z | \phi_{s'} \rangle = -s \delta_{s,-s'} i v k_z \mathcal{F}(k_z^2 \xi^2),$$

where $s, s' = \pm$ and $\mathcal{M}_{k_z}^0 = \rho_z \otimes \text{diag}(M_{k_z}^1, M_{k_z}^0, -M_{k_z}^0, -M_{k_z}^1)$, which leads to Eq. (1) in the main text.

APPENDIX C: ZERO-ENERGY SOLUTIONS FOR SMTI/SC HETEROSTRUCTURE

In this section, we calculate the zero-energy solutions for SMTI/SC heterostructure and the energy splitting due to their overlapping. In polar coordinates, by using the ansatz for the wave function $\Psi_{l,n}(r, \theta) = e^{i[l - \frac{1}{2}(\tau_z + \sigma_z)]\theta} \Psi_{l,n}(r)$, with l being an integer to make it single valued, we can separate angular and radial variables. The radial Hamiltonian is rewritten as $H_l(r) \Psi_{l,n}(r) = E_{l,n} \Psi_{l,n}(r)$, with

$$H_l(r) = \begin{pmatrix} h_l(r) & \Delta(r) \\ \Delta^*(r) & -\sigma_y h_{-l}^*(r) \sigma_y \end{pmatrix}, \quad (\text{C1})$$

where $h_l(r)$ is given by

$$h_l(r) = \begin{pmatrix} -\mu + M(r) & -ivD_r^l \\ -ivD_r^{1-l} & -\mu - M(r) \end{pmatrix}. \quad (\text{C2})$$

Due to the presence of the particle-hole symmetry $H_l = -\Xi H_{-l} \Xi^{-1}$ with $\Xi = \tau_y \sigma_y \mathcal{K}$, if E is an eigenvalue with the eigenfunction $\Psi_{l,E}(r) = [u_\uparrow, u_\downarrow, v_\downarrow, v_\uparrow]^T$, then $-E$ is also an eigenvalue and the corresponding eigenfunction is $\Psi_{-l,-E}(r) = [-v_\uparrow^*, v_\downarrow^*, u_\downarrow^*, -u_\uparrow^*]^T$. The zero-energy state only exists for $l = 0$ and needs to be an eigenstate of Ξ , i.e., $\Xi \Psi_{0,0}(r) = \zeta \Psi_{0,0}(r)$, which gives constraints on components of the eigenfunctions $u_\uparrow = -\zeta v_\uparrow^*$ and $u_\downarrow = \zeta v_\downarrow^*$. By redefining the spinors $u_\uparrow = \tilde{u}_\uparrow e^{-i\pi/4 - \zeta \int_0^r dr' \Delta(r')/\hbar v}$ and $u_\downarrow = \tilde{u}_\downarrow e^{i\pi/4 - \zeta \int_0^r dr' \Delta(r')/\hbar v}$, the four coupled differential equations in radial BdG equations are reduced to two real equations:

$$-[\mu - M(r)] \tilde{u}_\uparrow + v \partial_r \tilde{u}_\downarrow = 0,$$

$$v \left(\partial_r + \frac{1}{r} \right) \tilde{u}_\uparrow + [\mu + M(r)] \tilde{u}_\downarrow = 0. \quad (\text{C3})$$

For $0 < \mu < V_z$, by solution Eq. (C3), we find a solution localized at the vortex core,

$$\begin{pmatrix} u_\uparrow \\ u_\downarrow \end{pmatrix}_{\text{core}} \sim e^{-i\pi/4\sigma_z - \int_0^r dr' \frac{\Delta(r')}{\hbar v}} \begin{pmatrix} J_1(k_F r) \\ -J_0(k_F r) \end{pmatrix},$$

with the positive eigenvalue $\zeta = +1$ of Ξ and a bound state localized at the interface

$$\begin{pmatrix} u_\uparrow \\ u_\downarrow \end{pmatrix}_{\text{inter}} \sim \frac{e^{-i\pi/4\sigma_z}}{\sqrt{r}} e^{\int_R^r dr' \frac{\Delta(r')}{\hbar v}} \times \begin{cases} \left(\sqrt{\frac{\mu + V_z}{2V_z}} \right) e^{-\frac{\sqrt{m^2 - \mu^2}(r-R)}{\hbar v}}, & r > R, \\ \left(-\sin[k_F(r-R) - \delta + \frac{\pi}{4}] \right), \\ \left(\cos[k_F(r-R) - \delta + \frac{\pi}{4}] \right), & r < R, \end{cases} \quad (\text{C4})$$

with the negative eigenvalue $\zeta = -1$ of Ξ , where $\delta = \arctan \sqrt{\frac{V_z + \mu}{V_z - \mu}} + \frac{\pi}{4}$ is a phase determined by matching the wave function at the interface. To estimate the energy splitting for Majorana modes, we multiply $\langle \psi_{\text{core}} |$ to the BdG equation $H_0(r) |\Psi_+\rangle = E_+ |\Psi_+\rangle$, which yields $E_+ = \frac{\langle \psi_{\text{core}} | H_0(r) | \Psi_+\rangle}{\langle \psi_{\text{core}} | \Psi_+\rangle}$. Then using the relation $H_0(r) |\psi_{\text{inter}}\rangle = -iv \tau_z \sigma_x |\psi_{\text{inter}}\rangle \delta(r - R)$ and $H_0(r) |\psi_{\text{core}}\rangle = 0$, we arrive at the expression for the energy splitting for the zero mode in the main text [Eq. (4)].

- [1] F. Wilczek, Majorana returns, *Nat. Phys.* **5**, 614 (2009).
- [2] A. Stern, Non-Abelian states of matter, *Nature (London)* **464**, 187 (2010).
- [3] X. L. Qi and S. C. Zhang, Topological insulators and superconductors, *Rev. Mod. Phys.* **83**, 1057 (2011).
- [4] J. Alicea, New directions in the pursuit of Majorana fermions in solid state systems, *Rep. Prog. Phys.* **75**, 076501 (2012).

- [5] S. Q. Shen, *Topological Insulators*, Springer Series of Solid State Science Vol. 174 (Springer, Heidelberg, 2012).
- [6] C. W. J. Beenakker, Search for Majorana fermions in superconductors, *Annu. Rev. Condens. Matter Phys.* **4**, 113 (2013).
- [7] M. Sato and S. Fujimoto, Majorana fermions and topology in superconductors, *J. Phys. Soc. Jpn.* **85**, 072001 (2016).

- [8] R. M. Lutchyn, E. P. A. M. Bakkers, L. P. Kouwenhoven, P. Krogstrup, C. M. Marcus, and Y. Oreg, Majorana zero modes in superconductor–semiconductor heterostructures, *Nat. Rev. Mater.* **3**, 52 (2018).
- [9] A. Y. Kitaev, Fault-tolerant quantum computation by anyons, *Ann. Phys. (NY)* **303**, 2 (2003).
- [10] M. H. Freedman, A. Kitaev, M. J. Larsen, and Z. Wang, Topological quantum computation, *Bull. Am. Math. Soc.* **40**, 31 (2003).
- [11] C. Nayak, S. H. Simon, A. Stern, M. Freedman, and S. D. Sarma, Non-Abelian anyons and topological quantum computation, *Rev. Mod. Phys.* **80**, 1083 (2008).
- [12] L. Fu and C. L. Kane, Superconducting Proximity Effect and Majorana Fermions at the Surface of a Topological Insulator, *Phys. Rev. Lett.* **100**, 096407 (2008).
- [13] R. M. Lutchyn, J. D. Sau, and S. D. Sarma, Majorana Fermions and a Topological Phase Transition in Semiconductor-Superconductor Heterostructures, *Phys. Rev. Lett.* **105**, 077001 (2010).
- [14] Y. Oreg, G. Refael, and F. von Oppen, Helical Liquids and Majorana Bound States in Quantum Wires, *Phys. Rev. Lett.* **105**, 177002 (2010).
- [15] J. D. Sau, R. M. Lutchyn, S. Tewari, and S. Das Sarma, Generic New Platform for Topological Quantum Computation Using Semiconductor Heterostructures, *Phys. Rev. Lett.* **104**, 040502 (2010).
- [16] J. D. Sau, R. M. Lutchyn, S. Tewari, and S. Das Sarma, Robustness of Majorana fermions in proximity-induced superconductors, *Phys. Rev. B* **82**, 094522 (2010).
- [17] V. Mourik, K. Zuo, S. M. Frolov, S. R. Plissard, E. P. A. M. Bakkers, and L. P. Kouwenhoven, Signatures of Majorana fermions in hybrid superconductor-semiconductor nanowire devices, *Science* **336**, 1003 (2012).
- [18] A. Das, Y. Ronen, Y. Most, Y. Oreg, M. Heiblum, and H. Shtrikman, Zero-bias peaks and splitting in an Al–InAs nanowire topological superconductor as a signature of Majorana fermions, *Nat. Phys.* **8**, 887 (2012).
- [19] S. Nadj-Perge, I. K. Drozdov, J. Li, H. Chen, S. Jeon, J. Seo, A. H. MacDonald, B. A. Bernevig, and A. Yazdani, Observation of Majorana fermions in ferromagnetic atomic chains on a superconductor, *Science* **346**, 602 (2014).
- [20] J. P. Xu, M. X. Wang, Z. L. Liu, J. F. Ge, X. J. Yang, C. H. Liu, Z. A. Xu, D. D. Guan, C. L. Gao, D. Qian, Y. Liu, Q. H. Wang, F. C. Zhang, Q. K. Xue, and J. F. Jia, Experimental Detection of a Majorana Mode in the Core of a Magnetic Vortex inside a Topological Insulator-Superconductor $\text{Bi}_2\text{Te}_3/\text{NbSe}_2$ Heterostructure, *Phys. Rev. Lett.* **114**, 017001 (2015).
- [21] H.-H. Sun, K.-W. Zhang, L.-H. Hu, C. Li, G.-Y. Wang, H.-Y. Ma, Z.-A. Xu, C.-L. Gao, D.-D. Guan, Y.-Y. Li, C. Liu, D. Qian, Y. Zhou, L. Fu, S.-C. Li, F.-C. Zhang, and J.-F. Jia, Majorana Zero Mode Detected with Spin Selective Andreev Reflection in the Vortex of a Topological Superconductor, *Phys. Rev. Lett.* **116**, 257003 (2016).
- [22] L.-H. Hu, C. Li, D.-H. Xu, Y. Zhou, and F.-C. Zhang, Theory of spin-selective Andreev reflection in the vortex core of a topological superconductor, *Phys. Rev. B* **94**, 224501 (2016).
- [23] P. Zhang, K. Yaji, T. Hashimoto, Y. Ota, T. Kondo, K. Okazaki, Z. Wang, J. Wen, G. D. Gu, H. Ding, and S. Shin, Observation of topological superconductivity on the surface of an iron-based superconductor, *Science* **360**, 182 (2018).
- [24] D. Wang, L. Kong, P. Fan, H. Chen, S. Zhu, W. Liu, L. Cao, Y. Sun, S. Du, J. Schneeloch, R. Zhong, G. Gu, L. Fu, H. Ding, and H. J. Gao, Evidence for Majorana bound states in an iron-based superconductor, *Science* **362**, 333 (2018).
- [25] T. Machida, Y. Sun, S. Pyon, S. Takeda, Y. Kohsaka, T. Hanaguri, T. Sasagawa, and T. Tamegai, Zero-energy vortex bound state in the superconducting topological surface state of $\text{Fe}(\text{Se}, \text{Te})$, *Nat. Mater.* **18**, 811 (2019).
- [26] L. Y. Kong, L. Cao, S. Y. Zhu, M. Papaj, G. Y. Dai, G. Li, P. Fan, W. Y. Liu, F. Z. Yang, X. C. Wang, S. X. Du, C. Q. Jin, L. Fu, H.-J. Gao, and H. Ding, Tunable vortex Majorana zero modes in LiFeAs superconductor, *Nat. Commun.* **12**, 4146 (2021).
- [27] Q. Liu, C. Chen, T. Zhang, R. Peng, Y.-J. Yan, C.-H.-P. Wen, X. Lou, Y.-L. Huang, J.-P. Tian, X.-L. Dong, G.-W. Wang, W.-C. Bao, Q.-H. Wang, Z.-P. Yin, Z.-X. Zhao, and D.-L. Feng, Robust and Clean Majorana Zero Mode in the Vortex Core of High-Temperature Superconductor $(\text{Li}_{0.84}\text{Fe}_{0.16})\text{OHFeSe}$, *Phys. Rev. X* **8**, 041056 (2018).
- [28] W. Liu, L. Cao, S. Zhu, L. Kong, G. Wang, M. Papaj, P. Zhang, Y.-B. Liu, H. Chen, G. Li, F. Yang, T. Kondo, S. Du, G.-H. Cao, S. Shin, L. Fu, Z. Yin, H.-J. Gao, and H. Ding, A new Majorana platform in an Fe–As bilayer superconductor, *Nat. Commun.* **11**, 5688 (2020).
- [29] S. Zhu, L. Kong, L. Cao, H. Chen, M. Papaj, S. Du, Y. Xing, W. Liu, D. Wang, C. Shen, F. Yang, J. Schneeloch, R. Zhong, G. D. Gu, L. Fu, Y. Zhang, H. Ding, and H.-J. Gao, Nearly quantized conductance plateau of vortex zero mode in an iron-based superconductor, *Science* **367**, 189 (2020).
- [30] M. Li, G. Li, L. Cao, X. Zhou, X. Wang, C. Jin, C. K. Chiu, S. J. Pennycook, Z. Wang, and H.-J. Gao, Ordered and tunable Majorana-zero-mode lattice in naturally strained LiFeAs , *Nature (London)* **606**, 890 (2022).
- [31] C.-K. Chiu, T. Machida, Y. Huang, T. Hanaguri, and F.-C. Zhang, Scalable majorana vortex modes in iron-based superconductors, *Sci. Adv.* **6**, eaay0443 (2020).
- [32] E. J. König and P. Coleman, Crystalline Symmetry Protected Helical Majorana Modes in the Iron Pnictides, *Phys. Rev. Lett.* **122**, 207001 (2019).
- [33] R.-X. Zhang and S. Das Sarma, Intrinsic Time-Reversal-Invariant Topological Superconductivity in Thin Films of Iron-Based Superconductors, *Phys. Rev. Lett.* **126**, 137001 (2021).
- [34] M. Kheirkhah, Z. Yan, and F. Marsiglio, Vortex-line topology in iron-based superconductors with and without second-order topology, *Phys. Rev. B* **103**, L140502 (2021).
- [35] L.-H. Hu, X. Wu, C.-X. Liu, and R.-X. Zhang, Competing Vortex Topologies in Iron-based Superconductors, *Phys. Rev. Lett.* **129**, 277001 (2022).
- [36] A. P. Schnyder, S. Ryu, A. Furusaki, and A. W. W. Ludwig, Classification of topological insulators and superconductors, *Phys. Rev. B* **78**, 195125 (2008).
- [37] A. Kitaev, Periodic table for topological insulators and superconductors, in *Proceedings of the Advances in Theoretical Physics: Landau Memorial Conference*, AIP Conf. Proc. 1134 (AIP, Melville, NY, 2009), pp. 22–30.
- [38] C.-K. Chiu, J. C. Y. Teo, A. P. Schnyder, and S. Ryu, Classification of topological quantum matter with symmetries, *Rev. Mod. Phys.* **88**, 035005 (2016).

- [39] A. Haim and Y. Oreg, Time-reversal-invariant topological superconductivity in one and two dimensions, *Phys. Rep.* **825**, 1 (2019).
- [40] L. Fu and E. Berg, Odd-Parity Topological Superconductors: Theory and Application to $\text{Cu}_x\text{Bi}_2\text{Se}_3$, *Phys. Rev. Lett.* **105**, 097001 (2010).
- [41] F. Zhang, C. L. Kane, and E. J. Mele, Time Reversal Invariant Topological Superconductivity and Majorana Kramers Pairs, *Phys. Rev. Lett.* **111**, 056402 (2013).
- [42] X.-L. Qi, T. L. Hughes, and S.-C. Zhang, Topological invariants for the Fermi surface of a time-reversal-invariant superconductor, *Phys. Rev. B* **81**, 134508 (2010).
- [43] M. Sato, Topological odd-parity superconductors, *Phys. Rev. B* **81**, 220504(R) (2010).
- [44] D. A. Ivanov, Non-Abelian Statistics of Half-Quantum Vortices in p-Wave Superconductors, *Phys. Rev. Lett.* **86**, 268 (2001).
- [45] N. Read and D. Green, Paired states of fermions in two dimensions with breaking of parity and time-reversal symmetries and the fractional quantum Hall effect, *Phys. Rev. B* **61**, 10267 (2000).
- [46] M. Atiyah, and I. Singer, The index of elliptic operators on compact manifolds, *Bull. Am. Math. Soc.* **69**, 422 (1963).
- [47] R. Jackiw, and P. Rossi, Zero modes of the vortex-fermion system, *Nucl. Phys. B* **190**, 681 (1981).
- [48] R. Jackiw, and S.-Y. Pi, Chiral Gauge Theory for Graphene, *Phys. Rev. Lett.* **98**, 266402 (2007).
- [49] H. Zhang, C. X. Liu, X. L. Qi, X. Dai, Z. Fang, and S. C. Zhang, Topological insulators in Bi_2Se_3 , Bi_2Te_3 and Sb_2Te_3 with a single Dirac cone on the surface, *Nat. Phys.* **5**, 438 (2009).
- [50] M. Wimmer, Algorithm 923: Efficient numerical computation of the pfaffian for dense and banded skew-symmetric matrices, *ACM Trans. Math. Softw.* **38**, 1 (2012).
- [51] P. Hosur, P. Ghaemi, R. S. K. Mong, and A. Vishwanath, Majorana Modes at the Ends of Superconductor Vortices in Doped Topological Insulators, *Phys. Rev. Lett.* **107**, 097001 (2011).
- [52] C.-K. Chiu, M. J. Gilbert, and T. L. Hughes, Vortex lines in topological insulator-superconductor heterostructures, *Phys. Rev. B* **84**, 144507 (2011).
- [53] W. P. Su, J. R. Schrieffer, and A. J. Heeger, Soliton excitations in polyacetylene, *Phys. Rev. B* **22**, 2099 (1980).
- [54] A. Kitaev, Anyons in an exactly solved model and beyond, *Ann. Phys. (NY)* **321**, 2 (2006).
- [55] B. Zhou, H. Z. Lu, R. L. Chu, S. Q. Shen, and Q. Niu, Finite Size Effects on Helical Edge States in a Quantum Spin-Hall System, *Phys. Rev. Lett.* **101**, 246807 (2008).
- [56] J. Linder, T. Yokoyama, and A. Sudbø, Anomalous finite size effects on surface states in the topological insulator Bi_2Se_3 , *Phys. Rev. B* **80**, 205401 (2009).
- [57] E. J. Weinberg, Index calculations for the fermion-vortex system, *Phys. Rev. D* **24**, 2669 (1981).
- [58] T. Fukui and T. Fujiwara, Topological stability of majorana zero modes in superconductor-topological insulator systems, *J. Phys. Soc. Jpn.* **79**, 033701 (2010).
- [59] B. Roy and P. Goswami, Z_2 index for gapless fermionic modes in the vortex core of three dimensional paired Dirac fermions, *Phys. Rev. B* **89**, 144507 (2014).
- [60] J. C. Y. Teo and C. L. Kane, Majorana Fermions and Non-Abelian Statistics in Three Dimensions, *Phys. Rev. Lett.* **104**, 046401 (2010).
- [61] X.-L. Qi, T. L. Hughes, and S.-C. Zhang, Chiral topological superconductor from the quantum Hall state, *Phys. Rev. B* **82**, 184516 (2010).
- [62] A. R. Akhmerov, J. Nilsson, and C. W. J. Beenakker, Electrically Detected Interferometry of Majorana Fermions in a Topological Insulator, *Phys. Rev. Lett.* **102**, 216404 (2009).
- [63] L. Fu and C. L. Kane, Probing Neutral Majorana Fermion Edge Modes with Charge Transport, *Phys. Rev. Lett.* **102**, 216403 (2009).
- [64] J. C. Y. Teo and C. L. Kane, Topological defects and gapless modes in insulators and superconductors, *Phys. Rev. B* **82**, 115120 (2010).
- [65] X.-L. Qi, E. Witten, and S.-C. Zhang, Axion topological field theory of topological superconductors, *Phys. Rev. B* **87**, 134519 (2013).
- [66] J. Wang, Q. Zhou, B. Lian, and S.-C. Zhang, Chiral topological superconductor and half-integer conductance plateau from quantum anomalous Hall plateau transition, *Phys. Rev. B* **92**, 064520 (2015).
- [67] J. Wang, Electrically tunable topological superconductivity and Majorana fermions in two dimensions, *Phys. Rev. B* **94**, 214502 (2016).
- [68] B. Lian, X.-Q. Sun, A. Vaezi, X.-L. Qi, and S.-C. Zhang, Topological quantum computation based on chiral Majorana fermions, *Proc. Natl. Acad. Sci. USA* **115**, 10938 (2018).
- [69] Q. Yan, H. Li, J. Zeng, Q.-F. Sun, and X. C. Xie, A Majorana perspective on understanding and identifying axion insulators, *Commun. Phys.* **4**, 239 (2021).
- [70] K. T. Law, P. A. Lee, and T. K. Ng, Majorana Fermion Induced Resonant Andreev Reflection, *Phys. Rev. Lett.* **103**, 237001 (2009).
- [71] M. Cheng, R. M. Lutchyn, V. Galitski, and S. Das Sarma, Splitting of Majorana-Fermion Modes due to Intervortex Tunneling in a $p_x + ip_y$ Superconductor, *Phys. Rev. Lett.* **103**, 107001 (2009).
- [72] M. Cheng, R. M. Lutchyn, V. Galitski, and S. Das Sarma, Tunneling of anyonic Majorana excitations in topological superconductors, *Phys. Rev. B* **82**, 094504 (2010).
- [73] M. Mogi, Y. Okamura, M. Kawamura, R. Yoshimi, K. Yasuda, A. Tsukazaki, K. S. Takahashi, T. Morimoto, N. Nagaosa, M. Kawasaki, Y. Takahashi, and Y. Tokura, Experimental signature of parity anomaly in semi-magnetic topological insulator, *Nat. Phys.* **18**, 390 (2022).
- [74] J. Y. Zou, R. Chen, B. Fu, H. W. Wang, Z. A. Hu, and S. Q. Shen, Half-quantized Hall effect at the parity-invariant Fermi surface, *Phys. Rev. B* **107**, 125153 (2023).